ISSN 0016-7029, Geochemistry International, 2006, Vol. 44, No. 5, pp. 423–438. © Pleiades Publishing, Inc., 2006.
Original Russian Text © V.A. Alexeev, G.K. Ustinova, 2006, published in Geokhimiya, 2006, No. 5, pp. 467–482.

Solar Modulation of Galactic Cosmic Rays in the Three-Dimensional Heliosphere According to Meteorite Data

V. A. Alexeev and G. K. Ustinova

Vernadsky Institute of Geochemistry and Analytical Chemistry, Russian Academy of Sciences, ul. Kosygina 19, Moscow, 119991 Russia

e-mail: aval@icp.ac.ru

Received August 12, 2004

Abstract—Cosmogenic radionuclides with distinctive half-lives from chondritic falls were used as natural detectors of galactic cosmic rays (GCR). A unique series of uniform data was obtained for variations in the integral gradients of GCR with a rigidity of $R > 0.5$ GV in 1955–2000 on heliocentric distances of 1.5–3.3 AU and heliographic latitudes between 23° S and 16° N. Correlation analysis was performed for the variations in GCR gradients and variations in solar activity (number of sunspots, SS, and intensity of the green coronal line, GCL), the intensity of the interplanetary magnetic field (IMF), and the inclination of the heliospheric current sheet (HCS). Distribution and variations of GCR were analyzed in 11-year solar cycles and during a change in 22-year magnetic cycles. The detected dependencies of GCR gradients on the intensity of IMF and HCS inclination provided insight into the differences in the processes of structural transformation of IMF during changes between various phases of solar and magnetic cycles. The investigated relationships lead to the conclusion that a change of secular solar cycles occurred during solar cycle 20; moreover, there is probably still an increase in the 600-year solar cycle, which can be among the major reasons for the observed global warming.

DOI: 10.1134/S0016702906050016

INTRODUCTION

The investigation of the heliosphere, i.e., the area of solar activity, is among the main research fields of modern astrophysics. A remarkable feature of solar activity is its cyclic character, i.e., the quasi-periodical appearance and development of active areas. The most spectacular example of the solar cycle is the variations in the number of sunspots (SS) R_i with an average period of about 11 years [1] (Fig. 1). A good example for the influence of solar activity on processes in the heliosphere is the modulation of galactic cosmic rays (GCR) by solar wind: near the Earth, the intensity of GCR may decrease by an order of magnitude, anticorrelating with solar activity (which can be seen from the results of prolonged sounding in the stratosphere [2], Fig. 1). It is reasonable to expect that the boundary of GCR modulation corresponds to the dynamic boundary between solar wind and interstellar gas. Its position can be estimated from the gradient of GCR intensity in the heliosphere. In order to separate the galactic components of cosmic rays from the solar ones, spacecrafts for the measurement of their intensity were mainly launched in the years of the minimum solar activity, when the level of GCR intensity in the heliosphere was the highest. The results always suggested low, ~2–4%/AU, gradients of GCR with energies $E \geq 100$ MeV, which implied a tremendous size (>100 AU) of the modulation area [3], assuming that the modulating properties of the heliosphere are practically independent of the distance from the Sun. Indeed, owing to the superposition of temporal and spatial GCR variations, the measurements of their intensity, by the Pioneer 10, Voyager 1, and Voyager 2 spacecrafts in remote parts of the heliosphere (~20–50 AU), gave low gradients even in the years of maximum solar activity [4]. Moreover, measurements in the inner heliosphere (≤5 AU) were conducted near the ecliptic plane and did not provide reliable evidence for the existence of latitudinal gradients in GCR intensity. A new important step in the investigation of the heliosphere was related to the launch in October 1990 of the *Ulysses* spacecraft into a polar orbit. It was found [5] that the radial gradients of protons with $E > 2$ GeV became at least several times higher by increasing solar activity in the inner heliosphere. In contrast, latitudinal gradients appeared to be considerable in the years of the minimum of solar cycle 22 and decreased practically to zero in the southern latitudes with the development of cycle 23 in 1998–2001, when the heliocentric distance of the *Ulysses* decreased from 3 to 1.5 AU [5, 6]. Are these regularities transient or general? The answer to this question has a bearing on the character of the distribution and variations of GCR in the heliosphere, in particular, with respect to the properties and size of the modulation area. Nowadays, the necessary information on the character of these processes in the three-dimensional heliosphere over four

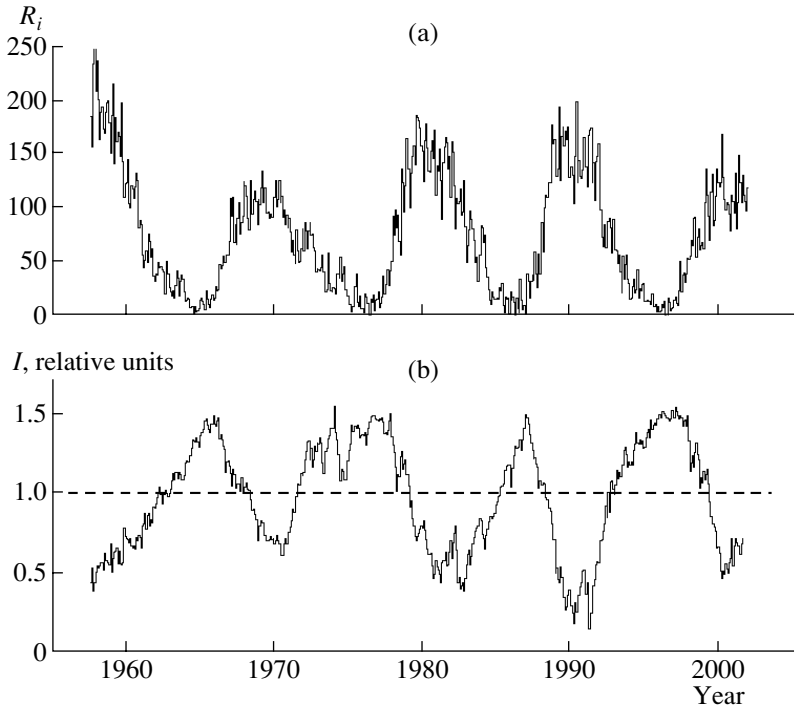

Fig. 1. Temporal variations in (a) the number of sunspots, R_i [1], and (b) the intensity of GCR with $R > 0.5$ GV in the stratosphere, I, [2].

solar cycles can be obtained only from meteorite studies.

WHAT DOES THEORY SUGGEST?

The standard models of modulation by solar wind assume that the flux of cosmic rays undergoes transport processes of diffusion through turbulent magnetic fields, convection processes owing to sweeping by magnetic fields frozen in the solar wind, and adiabatic cooling due to volume expansion of the solar wind with increasing distance from the Sun [7, 8]. A magnetic field, B, is usually specified as a sum of regular and random components; the former being responsible for the movement of particles along the field and the latter resulting in the resonance scattering of particles by turbulent elements, if the scale of turbulence is close to the Larmor radius of particles, $\rho = R/300B$. Although turbulent magnetic fields in the heliosphere scatter particles with a rigidity of up to several tens of GV, the regular magnetic field is sufficiently strong to provide anisotropic diffusion: particles diffuse more readily along the field than across it, i.e., $\varepsilon = \kappa_\perp/\kappa_\parallel \ll 1$, where $\kappa_\parallel$ and $\kappa_\perp$ are the diffusion coefficients along and across the field, respectively. The following equation of anisotropic diffusion describes the distribution of the density of charged particles (n) with rigidity R [8]:

$$\frac{\partial n}{\partial t} = \nabla_i(\kappa_{ik}\nabla_k n) - \nabla_i(un) + \frac{1}{3}\frac{\partial}{\partial R}(Rn)\nabla_i u, \qquad (1)$$

where u is the velocity of the solar wind, and κ_{ik} are the components of the generalized tensor of anisotropic diffusion in the form

$$\kappa_{ik} = \kappa_0\begin{pmatrix} 1 & 0 & 0 \\ 0 & \alpha_1 & \alpha_2 \\ 0 & -\alpha_2 & \alpha_1 \end{pmatrix}, \qquad (2)$$

where $\alpha_1 = R^2/(R^2 + 9 \times 10^4\Lambda^2B^2)$; $\alpha_2 = 300B\Lambda R(R^2 + 9 \times 10^4\Lambda^2B^2)$, and Λ is the transport path of the particles. The first term of Eq. (1) describes the diffusion of particles; the second term describes convection, and the third term describes adiabatic effects. Tensor (2) is given in the coordinate system with the $0x$ axis along the magnetic field and the $0y$ axis along the rotation axis of the Sun, and the ($x0z$) plane is the ecliptic. The diagonal components of the tensor describe the diffusion along and across the field. If the intensity of the regular magnetic field $B_0 = 0$, $\alpha_1 = 1$, and $\alpha_2 = 0$, then

$$\kappa_{ik} = \kappa_0\begin{pmatrix} 1 & 0 & 0 \\ 0 & 1 & 0 \\ 0 & 0 & 1 \end{pmatrix}, \qquad (3)$$

i.e., the diffusion becomes isotropic and κ_0 is the scalar coefficient of isotropic diffusion in the absence of a regular magnetic field. The off-diagonal antisymmetrical components $\pm\alpha_2$ in Eq. (2) depend on the direction of the magnetic field and describe the Hall effect or drift

of particles, the velocity of which may be comparable with that of solar wind. The direction of the drift depends on the polarity of the total solar magnetic field (TSMF) and the charge of the particles [9]. Since each ~11 yr near the maximum of solar activity, the polarity of TSMF changes, particles with charges of the same sign drift in opposite directions during the positive phase of a 22-year magnetic cycle (denoted as $A > 0$), when the magnetic-field lines of TSMF emanate from the northern polar area, and for the negative phase of a magnetic cycle ($A < 0$), when the field lines of TSMF enter into the northern polar area. When $A < 0$, the vectors of the magnetic moment and angular velocity of the Sun are opposite in direction, and positively charged particles drift along the HCS toward the Sun and from the equator to the poles of the heliosphere increasing the radial and decreasing the latitudinal gradients of GCR. When $A > 0$ the directions of these vectors coincide, and the opposite drift occurs from the poles to the equator and along the HCS away from the Sun, which decreases the radial gradients and increases the latitudinal gradients of GCR in heliosphere. Negatively charged particles drift in opposite directions. Thus, owing to the drift of protons in the heliosphere, their intensity must be higher in the positive phase of a magnetic cycle compared with the negative phase, which is observed in modern solar cycles [10].

The size of the modulation area depends on the solar-wind velocity, and, if it changes between the minimum and the maximum of solar activity, the size of the modulation area is also variable. The magnitude of GCR gradients in the heliosphere is directly connected to the problem of the upper boundary of the modulation area (r_0). Indeed, the depth of modulation (φ) and the radial gradient (G_r) of GCR are defined in standard models as

$$n(R) = n_0(R)\exp(-\varphi); \quad \varphi = \int_r^{r_0} \frac{u}{\kappa} d\xi; \qquad \text{and } G_r = \frac{1}{n}\frac{\Delta n}{\Delta r} = \frac{u}{\kappa}. \tag{4}$$

Consequently, the observed depth of modulation, φ, in the large modulating volume requires small GCR gradients, whereas large gradients may correspond to a small modulation area.

Given the considerable complexity of electromagnetic and magnetohydrodynamic conditions in the heliosphere, the most promising approach is to use numerical methods for the solution of equations of anisotropic diffusion and a database on the observed influence of solar activity on the model parameters. In particular, the steady-state solution to Eq. (1) accounting for the real heliolatitudinal distribution of solar activity and its variations with time derived from the data on GCR intensity [11] gives rise to the following important results [12–14]. The density of GCR increases with increasing heliolatitude, and the depth of

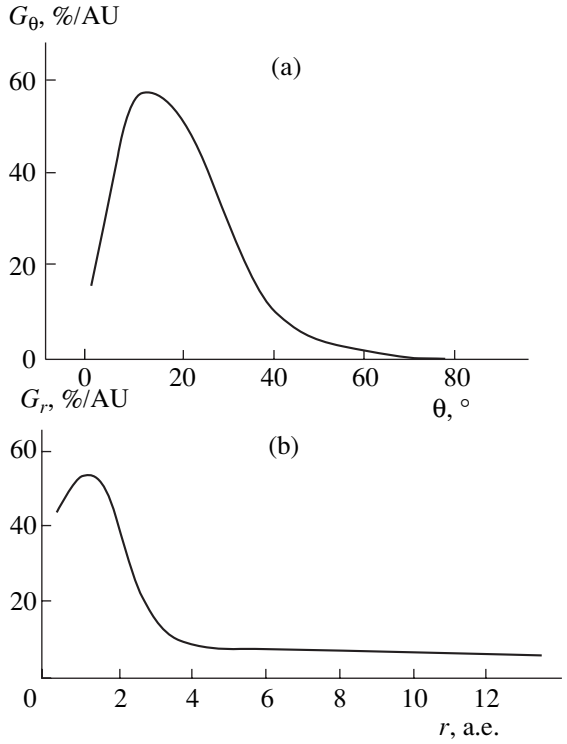

Fig. 2. (a) Heliolatitudinal variations in the lateral gradients G_θ and (b) spatial variations in the radial gradients G_r of GCR with energies $E \sim 1$ GeV (θ is measured relative to the helioequator) [14].

modulation decreases with increasing the distance from the Sun and increasing particle rigidity. This suggests that the modulation area is not spherical and there are considerable latitudinal gradients in GCR. The latitudinal gradients G_θ have different signs: they are negative and G_θ is from –3 to –5%/AU at latitudes of about ±10° (θ is measured from the helioequator) and positive at higher latitudes: at a distance of ~1 AU from the Sun they have maximum values of about 40–60%/AU in the range $\theta = \pm(10–25)°$ depending on the rigidity of particles. Figure 2a shows variations in latitudinal gradients for particles with the energy $E \sim 1$ GeV. It can be seen that G_θ increases up to 60%/AU at a maximum, and the area of G_θ occurrence reduces in the meridian plane to heliolatitudes of ±40° with maximum values within the θ range ±(10–25)°. Under such conditions, the radial gradients, G_r, are dependent on heliocentric distances. As can be seen in Fig. 2b, the maximum G_r values are observed at distances of ~2 AU, and up to ~85% of GCR intensity is restored to its level at a low-energy solar wind within ~3 AU from the Sun.

The data obtained suggest nonuniformity in the modulating properties of the heliosphere at various heliocentric distances and various heliographic latitudes. This allows us to introduce the concept of the area of effective GCR modulation as the zone of the maximum GCR gradient [15]. The gradient decreases

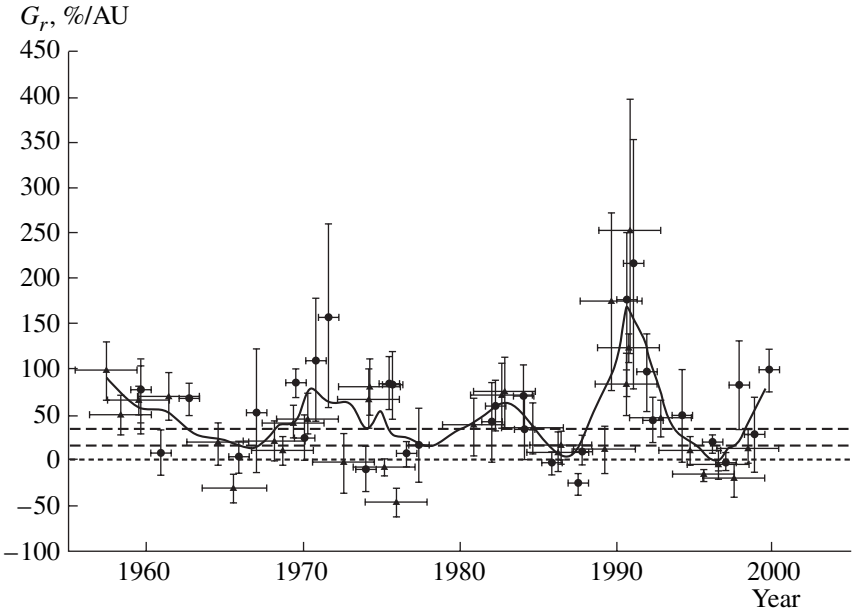

Fig. 3. Distribution and variations of the radial gradients of GCR with $R \geq 0.5$ GV, G_r, in the heliosphere in 1955–2000 derived from the data on the radioactivity of ^{54}Mn (circles), ^{22}Na (triangles), and ^{26}Al (dashed horizontal lines at 20–30%/AU) in 33 chondrites fallen to the Earth in 1959–2000. The curve was obtained by the double smoothing of experimental points using a first-order polynomial through five points [22].

to zero outside this area both toward and away from the Sun. Such an area corresponds to the zone of efficient deceleration of heterogeneous high-velocity solar-wind plasma. Therefore, its spatial position, shape, and size change depending on the level, phase, and character of solar activity [16], which was detected by modeling [8].

WHAT DOES THE EXPERIMENT SHOW?

Extensive investigations have accumulated, over many years, considerable experimental data on the measurement of GCR intensity in the solar system. These data include the results of neutron monitor studies, stratospheric measurements, concentrations of cosmogenic radionuclides in fallen meteorites, and direct measurements in interplanetary space. Various methods supplement each other and show some specific features, which provides an opportunity to explore cyclic changes in the intensity of GCR and their modulation by the Sun over more than four solar cycles. Neutron monitors record variations in high-energy GCR in near-Earth space, whereas episodic but more and more frequent spacecraft flights allow detection and investigation of an anomalous soft component of cosmic rays and spatial variations of GCR, although the superposition of spatial and temporal effects is inevitable. The long-term stratospheric measurements of ionizing radiation were launched in 1957 in Murmansk and Mirnyi [2, 17] and has provided a unique array of uniform data on the intensity of the primary component of GCR with the rigidity $R > 0.5$ GV in northern and southern latitudes during the past half century. The availability of these data enabled the development of a quantitative method for the analysis of the radioactivity of cosmogenic nuclides in meteorites in order to gain information on the intensity of GCR along meteorite orbits during various years of solar activity.

The use of meteorites with different inclinations and lengths of orbits as sounds for the determination of cosmic-ray variations in the heliosphere was proposed and developed in [15, 18]. Indeed, cosmogenic radionuclides with various half-lives, $T_{1/2}$, formed in meteorites are natural detectors of cosmic rays along meteorite orbits during ~$1.5T_{1/2}$ before the meteorite fall. Measuring the activity of a radionuclide at the moment of a meteorite fall provides insight into the average intensity of cosmic rays, I_r, for the average heliocentric distance of the meteorite, r, over a time period of ~$1.5T_{1/2}$. A comparison of I_r with the measured average intensity at 1 AU, I_1, for the same period (according to stratospheric data [2, 17]) allows estimation of radial gradients, G_r, using the equation (%/AU)

$$G_r(R > R_0) = (I_r/I_1 - 1)/(r - 1) \times 100\%, \qquad (5)$$

where R is the rigidity of particles in GV. Owing to the ablation of stony meteorites (chondrites) in the Earth's atmosphere, layers with an average shielding of ≥10 cm are accessible for radionuclide measurement, which corresponds to a particle rigidity of $R \geq 0.5$ GV. By investigating radionuclides with different $T_{1/2}$ in chondrites with different fall dates, lengths, and inclinations of orbits, a continuous data array can be obtained on the

distribution and variations of GCR with $R \geq 0.5$ GV in the three-dimensional heliosphere. The most convenient isotopes for these purposes are ^{54}Mn ($T_{1/2}$ = 300 d), ^{22}Na ($T_{1/2}$ = 2.6 yr), and ^{26}Al ($T_{1/2} = 7.4 \times 10^5$ yr) bearing information on the average intensity of GCR along the chondrite orbits during ~450 d, ~4 yr, and ~1 Myr, respectively, before the meteorite falls to Earth. This smoothes to a considerable extent both the temporal and spatial GCR variations along the meteorite orbits revealing the most important relationships.

Figure 3 presents the obtained data on the radial gradients of GCR with $R > 0.5$ GV along the orbits of the following chondrites (dates of the fall to Earth and aphelion, q', in AU are shown in parentheses): Pribram (7.04.59, 4.05), Bruderheim (4.03.60, 4.06), Harleton (30.05.61, 1.90), Peace River (31.03.63, 2.04), St. Severin (27.06.66, 1.97), Denver (15.07.67, 2.10), Lost City (3.01.70, 2.35), Malakal (15.08.70, ≥4), Kabo (25.04.71, 2.60), Guibga (26.02.72, 2.10), Gorlovka (17.07.74, ~1.9), Dhajala (28.01.76, 2.25), Jilin (8.03.76, 2.17), Innisfree (5.02.77, 2.76), Kutais (28.11.77, 1.98), Gujargaon (4.09.82, ≤1.9), Wethersfield (8.11.82, 2.37), Tomiya (22.08.84, 2.09), Binningup (30.09.84, 1.81), Kokubunji (29.07.86, 1.93), Trebbin (1.03.88, 1.97), Torino (18.05.88, 2.18), Tahara (26.03.91, 1.92), Noblesville (31.08.91, 1.92), Mbale (14.08.92, 2.51), Peekskill (9.10.92, 2.10), Mihonoseki (10.12.92, 1.95), Coleman (20.10.94, 3.12), Fermo (25.09.96, 1.97), El Hammami (10.08.97, ≥4), Kunya-Urgench (20.06.98, ~4), Hassilabyade (15.06.99, 1.90), and Moravka (6.05.00, 1.95) [15, 19–21]. The curve in Fig. 3 was obtained by the double smoothing of experimental points using a first-order polynomial for five points [22]. The meteorite database for the distribution and variations in the integral gradients of GCR ($R >$ 0.5 GV) in 1957–2000 characterizes heliocentric distances of 1.5–3.3 AU and heliolatitudes from 16° N to 23° S, which allows us to evaluate the dependence of the GCR modulation on the processes related to solar activity in the three-dimensional heliosphere during ≥4 solar cycles. For instance, a comparison of the meteorite data on variations in GCR gradients in 1957–2000 (Fig. 3) with the curve of variations in SS number [1] (Fig. 1) shows that the magnitude of gradients strongly depends on phases of the solar cycle, ranging from low and even negative values in the years of the minimum solar activity to ≥100%/AU in the years of the maximum activity [21]. The average gradients during the recent solar cycles (~20–30%/AU) are identical to the average gradients of the last million years, which indicates the constancy of the mechanism of solar GCR modulation at least within ~1 Myr [15]. The values obtained by all indirect methods are characterized by considerable uncertainties (≥100% in the meteorite method for large GCR gradients). Nonetheless, a series of uniform data with persistent large and small gradients in the years of maximum and minimum activity, respectively, over more than four solar cycles reflects a real regularity, i.e., correlation of GCR gradients with the level of solar activity. Strong variations in the GCR gradient depending on solar activity within 5 AU from the Sun was first detected during the flight of the *Ulysses* spacecraft [5]: radial gradients for protons with $E > 2$ GeV ranged from 0.5%/AU in the phase of the minimum solar activity in 1994–1996 to 5.3%/AU in the phase of the maximum solar activity in 1998–2001, i.e., the gradients increased by an order of magnitude. Measurements by Pioneer 10 and Pioneer 11 during the periods of the minimum solar activity within 5 AU from the Sun yielded radial gradients for protons with $E > 70$ MeV up to ~5%/AU [23]. At the increase in these values by one order of magnitude (modulation is much stronger within this energy range), gradients of about 50%/AU can be expected for the periods of the maximum solar activity, which is comparable with the meteorite data, taking into account the considerable uncertainties of the latter.

Since the 1970s, we have repeatedly pointed out [15, 24] that the high gradients obtained from meteorite data do not characterize the whole heliosphere, but suggest that a modulating layer of solar-wind magnetic heterogeneities efficiently scattering GCR is formed in the years of high solar activity within 2–3 AU from the Sun. Based on the regular variations in the solar modulation of GCR detected by the meteorite method, we formulated already more than 30 yr ago the concept of an effective modulating layer, i.e., established the heterogeneity of the structure and modulation properties of the heliosphere at various levels of solar activity [24, 25]. The layer develops within ~5 AU in the years of high solar activity and is probably a zone of interaction between the direct and inverse shock waves, high-velocity solar wind, and short-circuited flows of low-energy particles. It is characterized by the high turbulence of magnetic fields and high density of magnetic heterogeneities, which efficiently scatter GCR, producing an additional gradient of their intensity superposing on the low gradient typical of the low-velocity solar wind. Nonsteady-state processes attenuate with decreasing solar activity, and the layer reduces and thins out gradually moving toward the outer dynamic boundary of the modulation area. New modulating layers form with the development of new cycles. They shift during the expansion of the solar wind to remote heliocentric distances forming a chain of zones with high modulation properties (low diffusion coefficient) on the GCR path. During a minimum of solar activity, the residual modulation near the Earth is mainly controlled by the total volume of solar wind and shows on average small GCR gradients, which, however, are not constant and may be considerable in local segments of GCR pathways in the heliosphere.

This concept was strongly supported by the measurement of GCR with $E_p > 70$ MeV in 1984–1986 during the flight of Voyager 1 and Voyager 2 between 2 and 28 AU [26]. It was found that GCR intensity increases and decreases in a stepwise fashion, i.e., as if GCR have

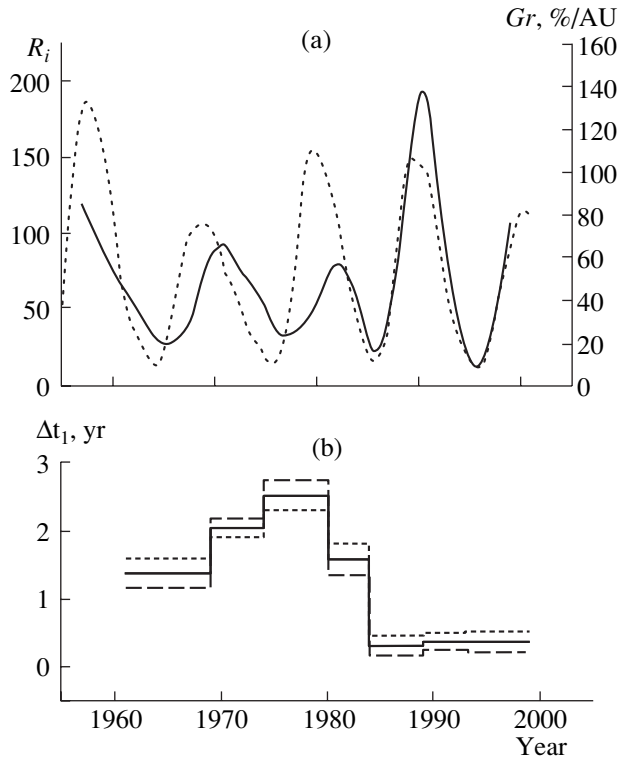

Fig. 4. (a) Smoothed curve of temporal variations in GCR gradients, G_r, compared with variations in the number of sunspots, R_i (dashed line), in 1957–2000; and (b) variations in the time lag between variations in GCR gradient and changes in the number of sunspots, Δt_1, in various time intervals for the maximum values of correlation coefficient, r_1; the dashed lines show standard deviation ($\pm 1\sigma$).

to overcome local segments or barriers with poor propagation conditions (low diffusion coefficients and high gradients). The gradients are small in the areas between the barriers. Steps on the intensity curves measured by spacecrafts can be adequately correlated with the steps on the curve of GCR intensity near the Earth (Fig. 1) taking into account a time lag for the processes in the heliosphere relative to active solar processes owing to the finite velocity of the solar wind. This implies that the barriers of the solar-wind heterogeneity encountered by GCR are not immovable, but propagate from the Sun toward the heliosphere boundary with solar-wind velocity and modulate new particle flows arriving from the Galaxy. Thus, GCR need to repeatedly overcome barriers on their way toward the Sun, and the extent of modulation in the 11-year cycles is controlled by the number and thickness of the barriers. Such a concept of modulation has been developed in [27–30] and other publications, and adequately reproduces the observed features of variations in GCR intensity and gradients.

Table 1. Time lag, Δt_1, between variations in GCR gradient and the number of sunspots in various time intervals for the maximum value of the correlation coefficient, r_1

Interval, years	Δt_1, yr	r_1
1957–1971	1.37 ± 0.21	0.83
1965–1977	2.04 ± 0.14	0.97
1971–1982	2.51 ± 0.21	0.87
1977–1986	1.57 ± 0.23	0.90
1982–1990	0.30 ± 0.15	0.96
1986–1996	0.36 ± 0.12	0.98
1990–1999	0.36 ± 0.15	0.99

It should also be noted that the meteorite data on GCR gradients refer not only to various heliocentric distances but to various heliographic latitudes and may include considerable latitudinal components of GCR gradients. They were first detected in the minimum of solar cycle 20 from the data on the radioactivity of the Dhajala and Innisfree chondrites with known orbits [31] and have been accurately measured during the *Ulysses* mission of 1996–2001 [5, 6]. The existence of latitudinal GCR gradients in the heliosphere suggests that the modulation area is not spherical and supports the above conclusions derived from the theory of anisotropic diffusion (Figs. 2a, 2b) [12–14]. The combined experimental and theoretical data suggest that the area of GCR modulation in the heliosphere is compressed in the meridian plane, mainly within heliolatitudes of $\pm 40°$, with the maximum gradients at heliolatitudes of $\pm(15–20)°$. Highly inclined meteorite orbits may extend beyond the modulation area at small distances from the Sun (1.5–3.3 AU), whereas the upper boundary of the modulation area (defined by the total volume of the solar wind) lies beyond ~50 AU near the helioequator plane [15, 18]. This model of the modulation area was first proposed in 1963 [32]. Given the possible latitudinal dependency of solar-wind velocity on the level of solar activity, the shape of the dynamic boundary of the modulation area and its distance from the Sun also depend on the phase of the solar cycle. During magnetically quiet periods, the projection of the boundary is an arc, whereas in the years of the maximum activity, it resembles a wing of a butterfly and is located farther from the Sun [15, 18].

CORRELATION ANALYSIS OF VARIATIONS IN SOLAR ACTIVITY ANG GCR GRADIENTS IN THE HELIOSPHERE

The many years of investigations of GCR modulation in the solar system and considerable progress in the understanding of the general mechanism of this phenomenon pose new questions indicating the complexity of mutual connection and coupling of dynamic processes in the Sun and three-dimensional heliosphere. Under conditions of a plasma state of solar material, its behavior is controlled by solar magnetic fields (SMF). The interaction of charged plasma with magnetic fields is a source of all the processes and phenomena on the Sun, which, taken together, make the concept of solar

activity. Owing to the high electric conductivity of solar plasma, magnetic fields are dragged away together with plasma by the solar wind into cosmic space forming the heliomagnetosphere. In fact, the structure and dynamics of the IMF are controlled by the structure and dynamics of solar magnetic fields. However, the discovery of scaling (scale invariance) of the intensity of IMF fluctuations in the frequency range 2.3×10^{-6} Hz during the Voyager 1 flight in 1980–1994, i.e., at a varying level of solar activity, at various heliocentric distances from 6.9 to 58.1 AU, and at heliographic latitudes ranging from –5.4° to 32.7° [30] posed a problem of the evaluation of the role of stochastic processes in GCR modulation. Of special significance for the searching, estimation, and distinguishing of the modulating effects of IMF perturbations is a rigorous analysis of the correlations between the distribution and variations of GCR in the heliosphere and various indexes of solar activity, primarily, the intensity of IMF. Perturbations of IMF (proportional to its intensity B [30]) change the diffusion coefficient of GCR, $\kappa \propto 1/B$, and control the degree of GCR modulation in various periods of solar activity (with convection, drift, and adiabatic cooling due to solar wind expansion) [7, 8]. The observed high coefficient of inverse correlation ($r \sim 0.8$–0.9) for a time shift of $\Delta t = 0$ between various components of GCR at 1 AU and B^2 even allows the calculation of B for the periods when the intensity of IMF was not directly measured [33]. The analysis of correlations is more problematic for other heliocentric distances, because of the absence of long series of uniform measurements of the intensity of GCR, the superposition of temporal and spatial GCR variations, and possible latitudinal variations in solar-wind velocity. However, the available meteorite data on GCR gradients (Fig. 3) allow us to perform such investigations for the heliosphere area up to ~4 AU, which is most susceptible to stochastic perturbations in IMF.

Figure 4a shows variations in the number of SS [1] compared with the smoothed curve of variations in GCR gradients during 1957–2000. Along with general positive correlations of the gradients with the level of solar activity, there are time lags, Δt_1, of the gradient variations relative to SS variations, especially large in 1970–1980, i.e., during the decline of the 20th and rise of the 21th solar cycles (such that in the minima of these cycles in 1976 and 1985, the lags differed by a factor of more than ≥8). As can be seen from Table 1, the correlation coefficients for these lags are ≥0.9. In

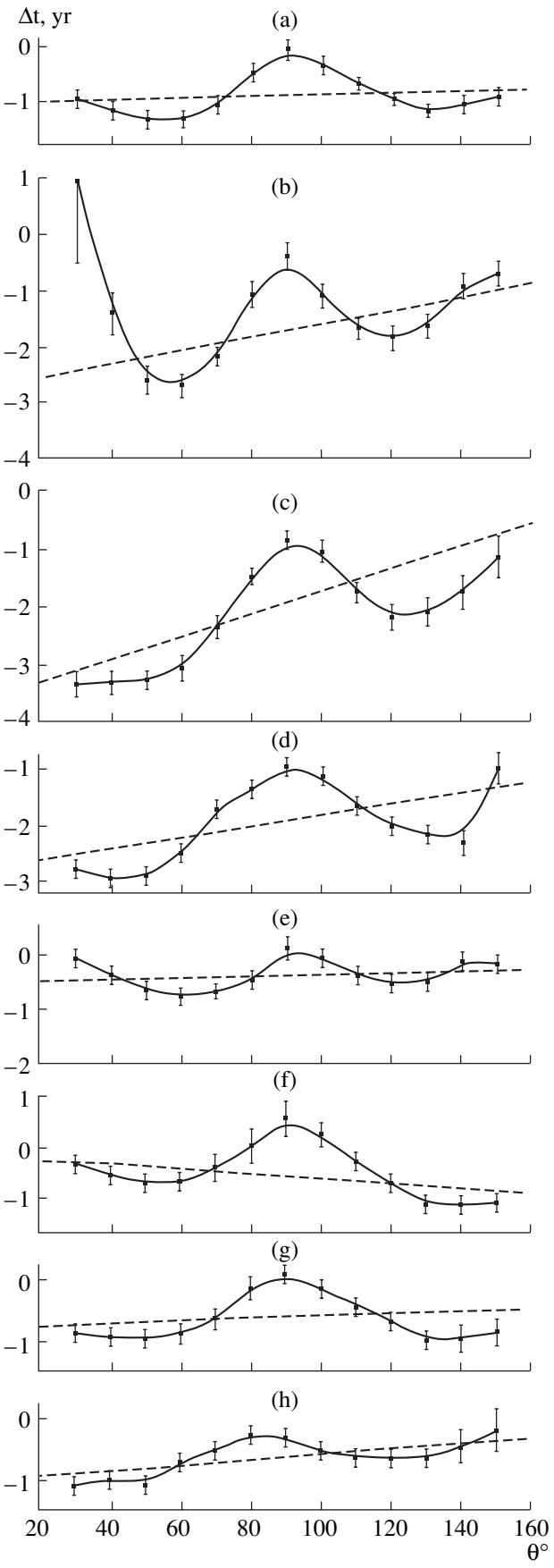

Fig. 5. Latitudinal variations in the time lag between variations in GCR gradients and changes in GCR intensity, Δt: (a) on average for the whole period (1957–1999) and for overlapping periods of the minimum and maximum solar activity during solar cycles 19–22: (b) 1957–1971; (c) 1965–1977; (d) 1971–1982; (e) 1977–1986; (f) 1982–1990; (g) 1986–1996; and (h) 1990–1999. The polar angle θ is measured from the north pole; the dashed lines are the regression lines whose parameters are given in Table 2; the intensity of GCL is given after [11].

Table 2. Parameters of the regression equation $\Delta t = a + b\theta$ for the relationships shown in Fig. 5

Interval, years	a	$10^{-3}b$
1957–1999	–1.06 ± 0.27	1.6 ± 2.7
1957–1971	–2.80 ± 0.56	12 ± 6
1965–1977	–3.66 ± 0.53	19 ± 6
1971–1982	–2.79 ± 0.46	9.7 ± 4.8
1977–1986	–0.63 ± 0.19	1.3 ± 2.0
1982–1990	–0.15 ± 0.31	–4.9 ± 3.1
1986–1996	–0.91 ± 0.32	1.9 ± 3.4
1990–1999	–1.00 ± 0.16	4.3 ± 1.8

1969–1971, the polarity of TSMF changed from minus to plus in northern latitudes [34], which marked the beginning of a new 22-year magnetic cycle. Figure 4b and Table 1 show that the maximum time lag of ~2.5 yr was observed for the positive phase of a magnetic cycle: $A > 0$ in 1970–1980, whereas for the subsequent negative phase of this magnetic cycle ($A < 0$ in 1980–1990), the time lag was only ~0.3 yr. As was mentioned above, the positive and negative phases of a magnetic cycle differ in the direction of drift of charged particles. When $A < 0$, positively charged particles drift from the equator to the poles of the heliosphere and along HCS toward the Sun, increasing the radial GCR gradients and decreasing the latitudinal GCR gradients. When $A > 0$, the opposite drift occurs from the poles to the equator and along HCS away from the Sun, which depresses the radial gradients and enhances the latitudinal gradients of GCR in the heliosphere. It is obvious that opposite convection flows encounter during these processes owing to the drift of particles and their sweeping by the solar wind, which strongly disturbs the ordering of processes in the heliosphere, in particular, the relation of GCR modulation to solar activity. According to [10], the relationship between GCR variations and parameters of solar activity is strongly disturbed during the periods of TSMF inversion (especially when a minus is changed by a plus in the northern hemisphere of the Sun). It is important that the time lags of GCR gradients relative to solar activity in the positive and negative phases of the above magnetic cycle are correlated with the duration of the periods of TMFS inversion during entering into these phases: $\Delta t_1 \sim 3$ yr in 1969–1971 and $\Delta t_1 \sim 1$ yr in 1980. It is interesting that the same time relationships were obtained for the hysteresis of GCR energy [35]: the spectra of particles become more rigid, probably owing to the acceleration of particles in the shock waves of turbulent processes triggered by the inversion [36].

Figure 5 presents latitudinal variations in the lag of GCR gradients relative to the intensity of GCL on average for the whole period of 1957–2000 (upper curve) and for the overlapping sequential periods of minimum and maximum solar activity during solar cycles 19–22 (polar angle θ is measured from the north pole). The dashed lines correspond to the regression parameters given in Table 2. On average, for the whole period of 1957–2000, the time lag is about one year, varying from the minimum value of 0.2 yr at the helioequator to the maximum values of ~1.2 yr at heliolatitudes of $\theta \sim 60°$ and 120° and again decreasing at higher latitudes. This corresponds to the observed evolution of solar activity and demonstrates its leading role in the structural development of the heliomagnetosphere. There are significant differences between the time lags for the maximum (periods of polarity reversals in TSMF) and minimum phases of various solar cycles. The longest lags accompanied by considerable north–south asymmetry were observed for the maximum of solar cycle 20: 3.03 yr for $\theta \sim 60°$ and 2.17 yr for $\theta \sim 120°$, which is probably related to a considerable structural rearrangement of the heliomagnetosphere, because of the strong (by a factor of more than ≥16) difference in the duration of polar reversals in the northern and southern latitudes during this period (Table 3). The effects of N–S asymmetry are illustrated by variations in the slope of the regression line $\Delta t = a + b\theta$ (Fig. 5): from a strong positive slope ($b \sim 0.019$) in the maximum of solar cycle 20 (1965–1977) to a negative slope ($b \sim -0.005$) in the minimum of solar cycle 21 (1982–1990). As can be seen from Table 2, the b value characterizing the slope of the regression line differs from zero for the whole database (1957–1999) within $\pm 1\sigma$, whereas this difference is as high as $\pm 2\sigma$ for the periods 1957–1982 and 1990–1999. During the transition from northern (small θ) to southern latitudes (high θ), the magnitude of the time lag, Δt, of variations in GCR gradients relative to variations in the intensity of GCL decreases at positive b values and increases at negative b values. These effects are considered below in more detail by an example of the 60° and 120° latitudes.

Figure 6a shows variations in the integrated gradients of GCR ($R > 0.5$ GV) along the meteorite orbits in 1957–2000 compared with the changes in GCL intensity at 60° and 120° according to [11]. Figure 6b (similar to Fig. 4b) exhibits a time lag between the GCR variations at 1.5–3.3 AU and changes in solar activity, which is especially strong for solar cycle 20 (Table 4). Noteworthy is the occurrence of N–S asymmetry in the time lag, $A_{NS} = [\Delta t_2(60°) - \Delta t_3(120°)]/[\Delta t_2(60°) + \Delta t_3(120°)] \times 100\%$ (Fig. 6c): at an average A_{NS} level of 17 ± 10% in 1957–1999, there is a tendency of A_{NS} to decrease ~10% in 1971–1982 ($A > 0$) and an about twofold increase in 1977–1986 ($A < 0$) after the TSMF inversion in the maximum of solar cycle 21 (Table 4). This is most likely related to the distinction between the inversion periods in the northern and southern hemispheres of the Sun. Indeed, the magnetic reversal occurred in February–November 1979 in the northern hemisphere and six months later, between October 1979 and May 1980, in the southern hemisphere [37] (Table 3). The analysis of inversion periods in solar cycles 18–22 showed that the 22-year magnetic cycles are not identical and differ in character and duration of

Table 3. Periods and duration (τ) of TSMF reversals in northern and southern latitudes according to the data of [37, 38]

Solar cycle	N			S		
	sign	period	τ, yr	sign	period	τ, yr
18	–/+	05.1950	0.08	+/–	12.1948–01.1949	0.17
19	+/–	02.1958–12.1959	1.92	–/+	07.1958	0.08
20	–/+	10.1969–01.1971	1.33	+/–	04.1970	0.08
21	+/–	02.–11.1979	0.83	–/+	09.1979–05.1980	0.75
22	–/+	01.1989–03.1990	1.25	+/–	08.1989–05.1991	1.83
23	+/–	11.1999–10.2000	1	–/+	06.1999–06.2001	2.08

the TSMF inversion in northern and southern latitudes: the inversions terminated earlier in the southern hemisphere at the maxima of solar cycles 18, 19, and 20 and in the northern hemisphere terminated at the maxima of solar cycles 21 and 22 [37, 38] (Table 3). This is undoubtedly related to the general level of activity in northern and southern latitudes: during seven 11-year cycles, up to cycle 20 inclusively, the activity in the northern hemisphere was higher than in the southern hemisphere [39]; however, the situation changed in 1981, when the southern hemisphere became more active than the northern hemisphere [40]. The different levels of solar activity in the northern and southern latitudes must be reflected in the asymmetry of GCR modulation. According to [41], the maximum asymmetry of $A'_{NS} \geq 1\%$ for particle flows with effective energies of 3–4 GeV was detected near the minimum of solar cycle 20. This is in agreement with the data derived from the Dhajala and Innisfree chondrites with known orbits for latitudinal GCR gradients ($R > 0.5$ GV) in 1973–1976: G_θ is ~ 3–5% per degree in southern latitudes and from –1.5 to 0.8% per degree in northern latitudes [15, 31, 42].

This effect is related to the peculiarity of the process of solar magnetic field rearrangement in solar cycle 20 [43]. Figure 7 shows the evolution of the lines of force for the regular solar magnetic field during various stages of magnetic reversal according to the data of [34]. It can be seen that the solar magnetic field was perfectly dipolar in 1967: the northern hemisphere was negative and the southern hemisphere, positive, such that the pattern was symmetrical relative to the north–south direction. The inversion began developing in March 1968 at heliolatitudes of 40°–50° in the southern hemisphere and propagated slowly toward the pole, which was reached in September 1969. In the northern hemisphere, the inversion began in the 40°–50° zone only in August 1970, but it was stronger and reached the pole within one year. During the whole period, the inversion was not observed in the near-equatorial zone, at ±40°. As can be seen in Fig. 7, the north–south asymmetry related to TSMF reversal existed from March 1968 to August 1971 and was most clearly manifested between September 1969 and August 1970, when the inversion of the magnetic field was already finished near the southern pole and had not yet began near the northern pole. Since no inversion occurred in the ±40° equatorial zone in 1969, charged particles could penetrate the heliosphere in southern latitudes along the magnetic field lines not only from the polar side but

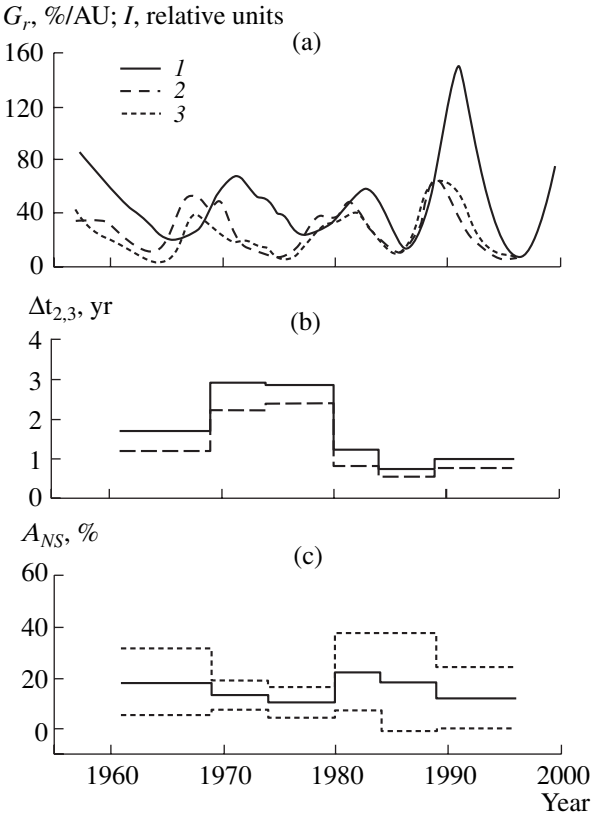

Fig. 6. Analysis of variations in GCR gradients (G_r) and GCL intensity (I): (a) a comparison of variations in GCR gradients (*1*) and GCL intensity for polar angles of θ = 60° (*2*) and θ = 120° (*3*); (b) time lags Δt_2 (θ = 60°, solid line) and Δt_3 (θ = 120°, dashed line) between variations in GCR gradients and changes in the intensity of GCL in various time intervals for the maximum values of correlation coefficients, r_2 and r_3, respectively; (c) north–south asymmetry (A_{NS}) of time lags for θ = 60° and θ = 120°: $A_{NS} = [\Delta t_2 - \Delta t_3]/[\Delta t_2 + \Delta t_3] \times 100\%$ (solid line); the dashed lines show standard deviation (±1σ).

Table 4. Values of time lags, Δt_2 and Δt_3, between variations in GCR gradients and changes in GCL intensity at $\theta = 60°$ and $\theta = 120°$ in various time intervals for the maximum values of correlation coefficients, r_2 and r_3, respectively

Interval, years	GCL, $\theta = 60°$		GCL, $\theta = 120°$		A_{NS}, %
	Δt_2, yr	r_2	Δt_3, yr	r_3	
1957–1971	1.69 ± 0.28	0.58	1.18 ± 0.23	0.78	18 ± 13
1965–1977	2.90 ± 0.20	0.91	2.22 ± 0.19	0.88	13 ± 6
1971–1982	2.86 ± 0.22	0.90	2.36 ± 0.21	0.90	10 ± 6
1977–1986	1.21 ± 0.24	0.86	0.78 ± 0.16	0.95	22 ± 15
1982–1990	0.73 ± 0.21	0.90	0.51 ± 0.10	0.97	18 ± 19
1986–1996	0.97 ± 0.17	0.96	0.77 ± 0.13	0.97	12 ± 12
1957–1999	1.23 ± 0.16	0.72	0.88 ± 0.12	0.87	17 ± 10

also in the near-equatorial zone at ≤40° S [43]. In northern latitudes, charged particles had such an opportunity only starting from August 1970 and, especially, in 1971, when the polarity of the magnetic field changed at the northern pole. From that moment, the solar magnetic field restored its N–S symmetry. However, a comparison of the first and last panels of Fig. 7 suggests that the inversion of TSMF resulted in that the heliosphere appeared to be open not only near the poles, as in 1967, but also in the part in the near-equatorial zone at ±40°. This additional possibility for the penetration of charged particles into the heliosphere through a kind of hole in the magnetosphere was probably responsible for the rapid increase in GCR intensity at the end of 1971 and for the general higher level of GCR intensity in solar cycle 20 compared with cycle 19 [43]. In fact, TSMF can probably have such configurations when, instead of a single neutral current sheet, there is one neutral sheet and two neutral cones at heliolatitudes of ±40°, which may play a key role if the processes of drift are predominant [44]. The reverse drift of particles after the termination of solar magnetic field rearrangement

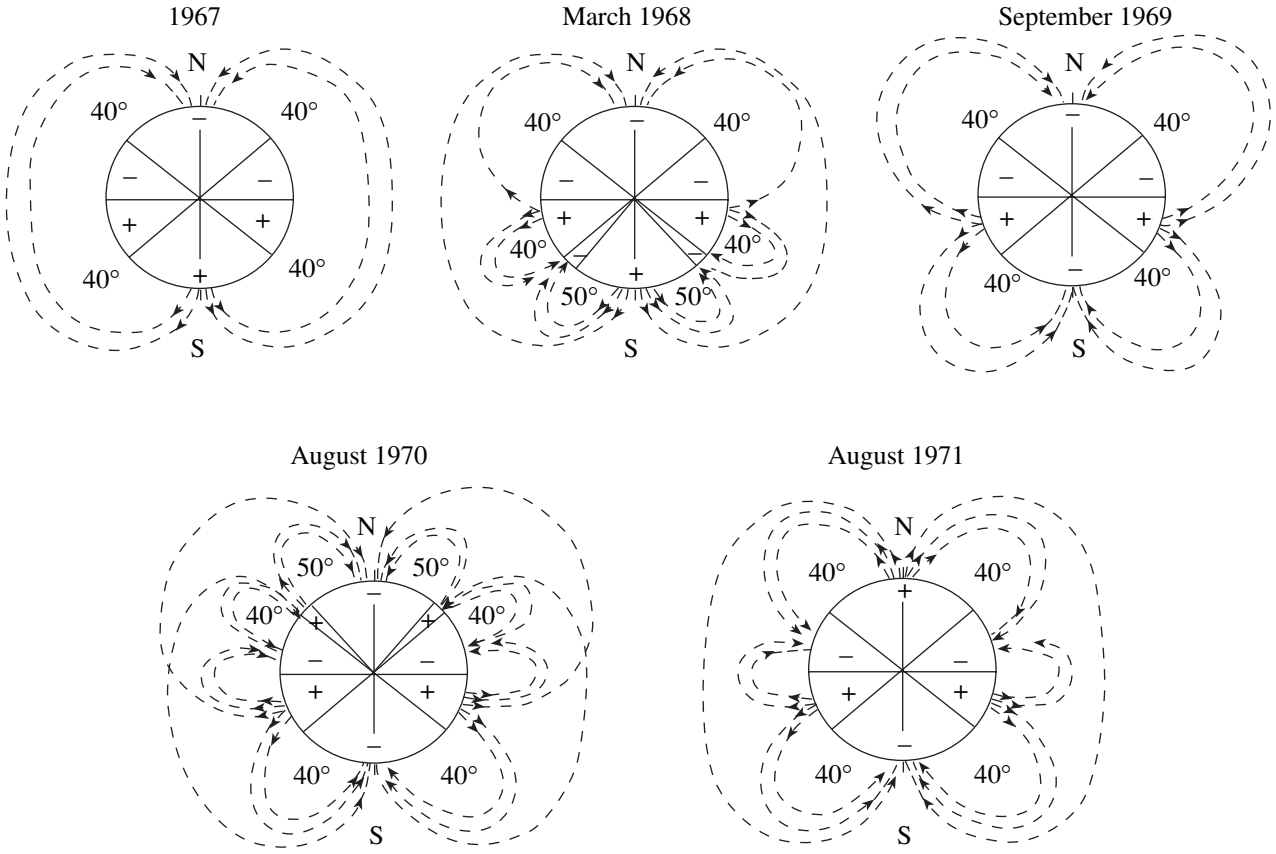

Fig. 7. Evolution of solar magnetic fields in 1967–1971 [43] (according to the data of [34]).

in northern latitudes in August 1971 could be the reason for the increase of GCR intensity in the northern hemisphere up to negative gradient values. Owing to the different character and duration of inversion periods during the changes of various phases of magnetic cycles, the N–S asymmetry must occur differently in the different cycles. In fact, according to [41] A'_{NS} fluctuates near zero in the negative phases of magnetic cycles.

Our analysis shows that the influence of solar activity variations on the spatial distribution and modulation of GCR in the heliosphere is indirect: in agreement with this theory it occurs through the influence on the structure and disturbance of IMF. It is reasonable, therefore, to pose the question on the correlations of GCR gradients with the intensity of IMF. Figure 8a compares variations in the radial gradients of GCR (curve *1*) with variations in the intensity of IMF, *B* [45] (curve *2*). There is a positive correlation between radial gradients of GCR at about 2–4 AU with IMF intensity. However, this correlation is different for different solar cycles and for the ascent and descent periods of solar cycles. The time lag, Δt_4, between the GCR gradients and variations in IMF intensity fluctuates near zero during the descent periods of solar cycles 21 and 22 (i.e., independent of the phase of magnetic cycle) with a very high correlation coefficient of $r_4 \geq 0.9$ (Fig. 8b, Table 5). However, during the ascent phase of cycle 22, an increase in GCR gradients is enhanced by the drift of particles from the heliosphere at a high inclination of HCS [46] (Fig. 9) and is even faster than an increase in the intensity of IMF. These regular relations are disturbed again by solar cycle 20 and the magnetic cycle of 1969–1981 as a whole: there is a poor correlation between the gradients and IMF; the time lag is $\Delta t_4 > 1.5$ yr at $r_4 \sim 0.5$. The important role of HCS inclination in the development of solar activity and GCR modulation is evident. As can be seen from Table 6, changes in HCS inclination are primary, i.e., changes in SS or IMF are retarded with respect to changes in HCS. However, the time lag between SS and HCS variations is small: the average value is $\Delta t_6 = 0.22 \pm 0.12$ yr (for all intervals except for 1990–2001, Δt_6 for SS does not differ from 0 within 1σ, i.e., HCS and SS change almost synchronously). The development and changes in IMF are retarded with respect to changes in solar processes on average by one year (Fig. 9b). The main factor of the influence of HCS on the modulation of GCR is constraining the direction of the particle drift. It is clearly seen from Fig. 9a that the slope of HCS strongly correlates with solar activity, varying from $\alpha < 10°$ at a minimum of solar activity to $\alpha > 70°$ at the maximum. Near solar activity maxima, high-latitude drift flows cause the strongest perturbations in the heliomagnetosphere, preventing GCR penetration. Figure 9c displays a strong correlation ($r_5 = 0.96$, Table 5) between the magnitude of radial GCR gradients and the inclination of HCS during a change of the magnetic cycle near the maximum of solar cycle 22 in 1990. It was noted at the beginning of this paper that,

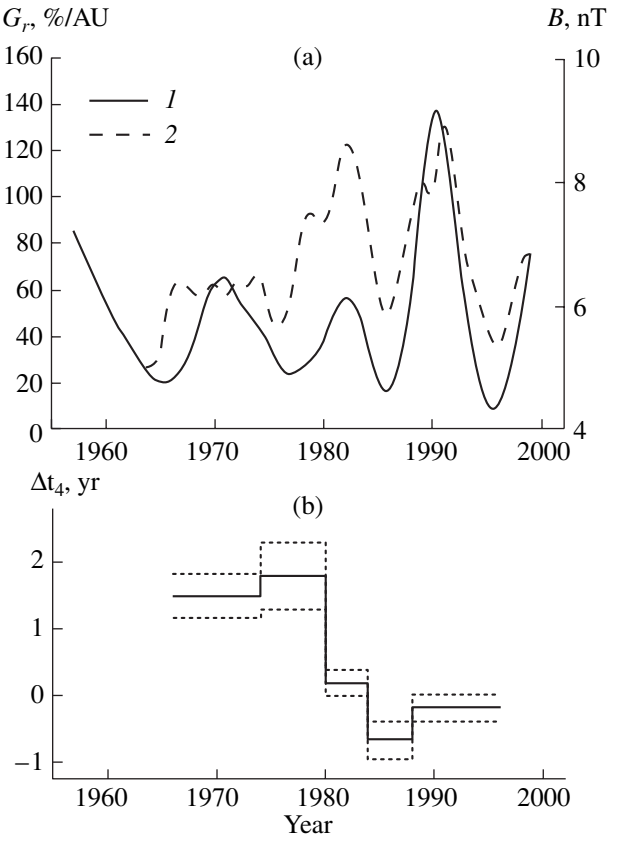

Fig. 8. (a) Comparison of variations in radial GCR gradients (G_r, curve *1*) with variations in the intensity of IMF [45] (*B*, curve *2*); (b) time lag between variations in GCR gradients and changes in IMF intensity in various time intervals; the dashed lines show standard deviation $\pm 1\sigma$.

according to the measurements by the *Ulysses* spacecraft, the radial gradients of protons with $E > 2$ GeV became several times higher in that time period [5]. The relationships shown in Fig. 9c suggest that this effect was not accidental; it was observed over three solar maxima near 1980, 1990, and 2000 and resulted from both an increase in IMF disturbance (Fig. 9b) and high inclination of HCS.

Table 5. Values of time lags, Δt_4 and Δt_5, between variations in GCR gradients and changes in the IMF intensity and HCS inclination in various time intervals for the maximum values of correlation coefficients, r_4 and r_5, respectively

Interval, years	IMF		HCS	
	Δt_4, yr	r_4	Δt_5, yr	r_5
1965–1977	1.48 ± 0.33	0.57	–	–
1971–1982	1.78 ± 0.41	0.41	–	–
1977–1986	0.18 ± 0.20	0.94	1.65 ± 0.34	0.78
1982–1990	-0.67 ± 0.29	0.76	0.20 ± 0.14	0.97
1986–1996	-0.19 ± 0.20	0.89	0.57 ± 0.13	0.96
1990–1999	–	–	0.70 ± 0.16	0.96

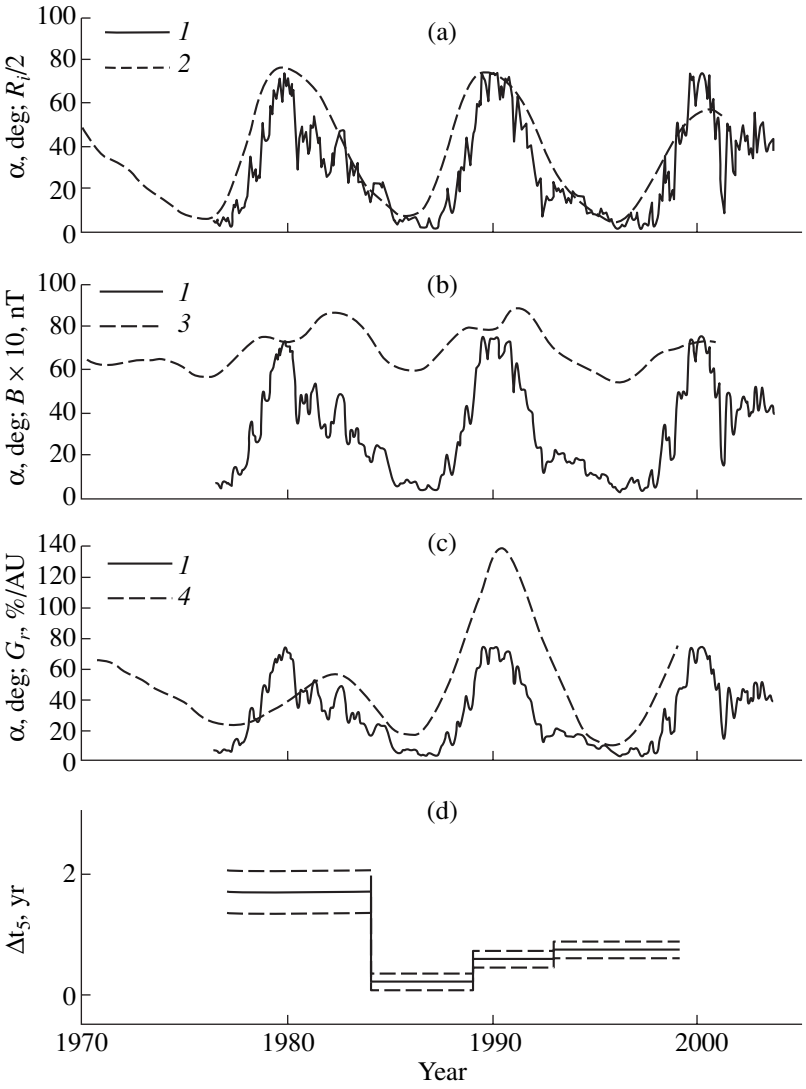

Fig. 9. Comparison of the variations in the inclination of HCS [46] (α, curve *1*) with (a) variations in the number of sunspots [1] (curve *2*), (b) IMF intensity [45] (*B*, curve *3*), and (c) GCR gradient (G_r, curve *4*); (d) time lag between variations in GCR gradients (Δt_5) and changes in the inclination of HCS in various time interval for the maximum value of correlation coefficient, r_5.

Unfortunately, there is no evidence for the inclination of HCS during solar cycle 20. However, even in the neighboring 21th cycle, the correlation with GCR gradients is less distinct: $\Delta t_5 \sim 1.65$ at $r_5 = 0.78$ near the maximum of this cycle in contrast to $\Delta t_5 \sim 0.57$ with $r_5 = 0.96$ for the maximum of cycle 22 (Table 5, Fig. 9d). It should be noted that various anomalous features of cycle 20 have already been discussed for almost 30 years [47], and there is no reason to suppose a violation of data uniformity related to IMF measurements before 1973. In contrary, the presented analysis of the correlations between GCR gradients and solar activity indexes, characteristics of N–S asymmetry, and the weakening of correlations with IMF in 1969–1981 provide compelling evidence for a deep structural rearrangement of IMF in this period, which was probably related to the change of a secular cycle of solar activity. Such a period (80 ± 50 y) is characteristic of quasi-periodic variations in the height of the maxima of 11-year cycles [48]. In contrast to the 11-year cycles connected with the frequency of solar activity phenomena, the secular cycle reflects mainly variations in their intensity. Figure 10a shows variations in the maximum average annual relative number of SS in 1700–2001 smoothed by the Gleisberg method [49]. It can be seen that the secular cycle minima coincided with solar cycles 6 and 14, and maxima, with cycles 3 and 9, and the change of the previous secular cycle coincided with cycle 20. The most intense occurrences of solar activity were observed during solar cycles 18–21: the highest values of maximum Wolf numbers, the widest zones of SS groups, the clearest distinguishing of active latitudes, etc.

An important feature of secular modulation is the periodic asymmetry in the activity of the northern and southern hemispheres of the Sun [50]. The activity level in the northern and southern hemispheres is approximately the same for extremely high and extremely low amplitudes of the 11-year cycles, whereas cycles of moderate intensity show maximum asymmetry [51]. As was mentioned above, a change in the intensity of solar activity in the northern and southern hemispheres happened at the boundary between cycles 20 and 21. The curve of the secular cycle (Fig. 10a) has a character of free harmonic oscillations, which could be due to cyclic variations in the depth of the convection zone of the Sun [39]. The existence of cycles longer than 100 yr is also possible. For instance, the historical record of sunspots and auroras suggests the existence of a 600-year cycle. The positive slope of the regression line may be indicative of the change of a 600-year cycle of solar activity in cycle 20 (it is also possible that this change will occur in the nearest cycles). The plausibility of this suggestion will be assessed by future studies. If this cycle is still in its ascent phase, this factor could contribute to the observed global warming. Figure 10b shows variations in temperature (T) in the lower atmosphere during the past 150 yr [52]. There is a clear tendency of T to increase with time. A similar tendency can be observed for variations in CO_2 concentration in the Earth's atmosphere, although the correlation with temperature has been disturbed in several segments of the time scale [53]. The analysis of regression lines in Figs. 10a and 10b gives a rate of SS increase of 0.22%/yr and a rate of T increase of only 0.0015%/yr. The difference in the increase rates is related to at least two natural reasons. First, the temperature of the Earth is affected by the Sun's radiative energy, which depends on solar activity; whereas the SS number is only a formal index of solar

Table 6. Values of time lags, Δt_6 and Δt_7, between variations in the number of sunspots and changes in IMF intensity and HCS inclination in various time intervals for the maximum values of correlation coefficients, r_6 and r_7, respectively

Interval, years	Sunspots		IMF	
	Δt_6, yr	r_6	Δt_7, yr	r_7
1976–1986	0.14 ± 0.16	0.98	1.28 ± 0.28	0.70
1981–1990	0.06 ± 0.18	0.94	0.93 ± 0.37	0.62
1986–1996	0.19 ± 0.18	0.95	0.60 ± 0.20	0.81
1990–2001	0.53 ± 0.14	0.96	1.00 ± 0.20	0.80
1976–2001	0.22 ± 0.12	0.92	0.93 ± 0.21	0.70

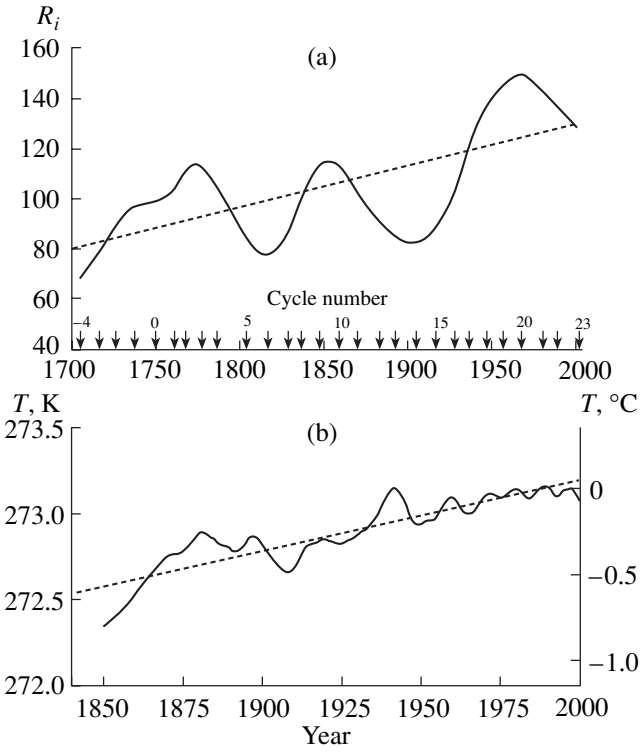

Fig. 10. (a) Secular cycles of solar activity in 1700–2001 (solid curve); R_i are the values of the maximum annual average Wolf number in the 11-year cycles smoothed by the Gleisberg method [49]; the maxima of the cycles are marked by arrows; (b) variations in the temperature of the Earth's lower atmosphere during the past 150 yr according to [52] (solid line); the dashed lines are regression lines: (a) $y = -203 + 0.166x$ and (b) $y = 265 + 0.0042x$.

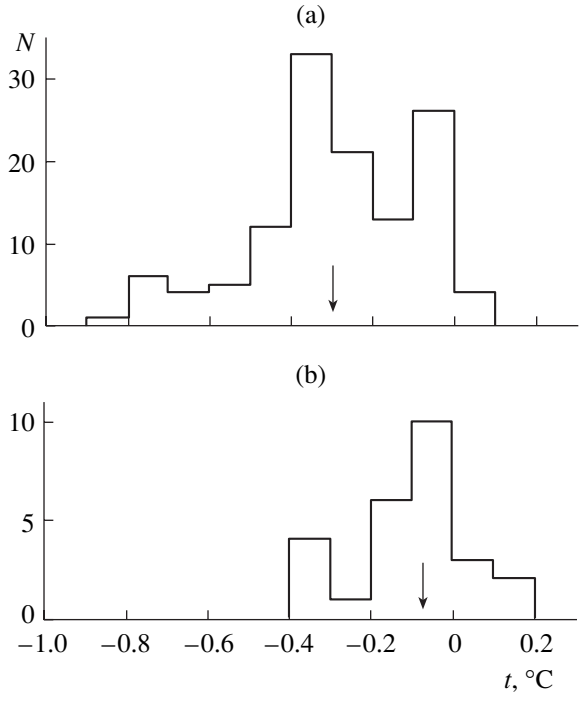

Fig. 11. Distribution of the average annual temperatures of the Earth's lower atmosphere, t, in 1850–2000 for years with different average numbers of sunspots: (a) $N < 100$ and (b) $N \geq 100$. The arrows show the median values of the temperature: (a) $t_{med} = -0.30 \pm 0.02$ and (b) $t_{med} = -0.075^{+0.065}_{-0.045}$; standard errors ($\pm 2\sigma$) were calculated by the nonparametric method of data processing [54].

activity, which is not directly related to the temperature. It is reasonable to expect that inertial processes on the Sun result in a strong smoothing of solar activity variations and diminish an increase in its luminosity. Second, in a similar manner, the high inertia of terrestrial processes, in particular, inertial processes in the ocean strongly decelerate and, fortunately, mitigate the temperature increase on a long time scale. Nonetheless, a definite correlation between the Earth's temperature and solar activity can be seen in Figs. 11a and 11b, which show the distribution of the average annual temperatures in the lower atmosphere in 1850–2000 for years with different average numbers of SS: (a) $N < 100$ and (b) $N \geq 100$. The arrows indicate the median values of temperature: $t_{med} = -0.30 \pm 0.02$ and $t_{med} = -0.075^{+0.065}_{-0.045}$ in degrees centigrade, i.e., the average temperature of the Earth's lower atmosphere is higher in the years of higher solar activity ($N \geq 100$). It is interesting that this effect is observed at small delays of the temperature relative to SS (several years) and is leveled out at high delays (tens of years), which demonstrates the inertial mechanism of natural processes: a relatively rapid response of temperature in the lower atmosphere on the level of solar activity and slow smoothing of temperature fluctuations on a long time scale (~100 yr) owing primarily to the tremendous inertial potential of the ocean. Thus, our analysis indicates that solar activity is one of the main natural factors affecting the climate of the Earth.

CONCLUSIONS

Processes on the Sun and solar activity are the major control of processes in the heliosphere through formation and disturbances in the IMF. This is manifested on the most global scale in the solar modulation of GCR, i.e., variations in GCR intensity at various heliocentric distances and in various heliographic latitudes are in agreement with the varying level of solar activity. It is clear that GCR intensity is a fine tool for the investigation of the electromagnetic structure of the heliosphere and its changes related to solar activity variations. However, such investigations require long series (several 11-year solar cycles) of uniform data on GCR intensity in interplanetary space. At present, only the natural detectors of GCR, radionuclides with various half-lives in chondrites that fell to the Earth in 1959–2000, provide such data on GCR intensity within 2–4 AU from the Sun over more than four solar cycles. The correlation analysis of these parameters with various indexes of solar activity (SS number and GCL intensity), inclination of HCS, and IMF intensity leads to the conclusion that the change of a secular cycle occurred in solar cycle 20 (1965–1976) and caused strong electromagnetic disturbances in the heliosphere. The positive slope of the regression line of secular cycles in Fig. 10a suggests that the current 600-year or longer solar cycle is still in its ascent phase, which could contribute to the observed warming of the Earth's climate. Indeed, the correlation analysis of variations in solar activity and the temperature of the Earth's lower atmosphere over the past 150 years leads to the conclusion that solar activity must be regarded as one of the main factors controlling the Earth's climate.

ACKNOWLEDGMENTS

The authors are grateful to Yu.A. Shukolyukov for his favorable and constructive review of the manuscript.

REFERENCES

1. http://www.sunspot.net/cat3sun_r.html
2. G. A. Bazilevskaya, M. B. Krainev, Yu. I. Stozhkov, et al., "Long-Term Soviet Program for the Measurement of Ionizing Radiation in the Atmosphere," J. Geomagn. Geoelectr. **43**, 893–900 (1991).
3. F. McDonald, H. Moraal, J. P. L. Reinecke, et al., "The Cosmic Radiation in the Heliosphere at Successive Solar Minima," J. Geophys. Res. **97**, 1557–1570 (1992).
4. D. Venkatesan, R. B. Decker, and S. M. Krimigis, "Cosmic Ray Intensity Gradients in the Radial Distance 1–13 AU as Determined from a Comparative Study of Observations by Spacecrafts 'Voyagers-1 and -2,' and Earth-Orbiting Satellite IMP-8," in *Proceedings of 18th International Cosmic Ray Conference, Bangalore, India, 1983* (Bangalore, 1983), Vol. 10, pp. 156–159.
5. A. V. Belov, E. A. Eroshenko, B. Heber, et al., "Latitudinal and Radial Variation of >2 GeV/N Protons and α-Particles in the Southern Heliosphere at Solar Maximum: ULYSSES COSPIN/KET and Neutron Monitor Network Observations," in *Proceedings of 27th International Cosmic Ray Conference, Hamburg, 2001* (Hamburg, 2001), pp. 3996–3999.
6. F. McDonald, Z. Fujii, P. Ferrando, et al., "The Cosmic Ray Radial and Latitudinal Intensity Gradients in the Inner and Outer Heliosphere 1996-2001.3," in *Proceedings of 27th International Cosmic Ray Conference, Hamburg, Germany, 2001* (Hamburg, 2001), pp. 3906–3909.
7. E. N. Parker, *Interplanetary Dynamical Processes* (Interscience, New York, 1963; Mir, Moscow, 1965).
8. L. I. Dorman, *Variations in Galactic Cosmic Rays* (Mosk. Gos. Univ., Moscow, 1975) [in Russian].
9. J. R. Jokipii, E. H. Levy, and W. B. Hubbard, "Effects of Particle Drifts on Cosmic Ray Transport. 1. General Properties, Application to Solar Modulation," Astrophys. J. **213**, 861–868 (1977).
10. G. A. Bazilevskaya, Yu. I. Stozhkov, and T. N. Charakhch'yan, "Variations in Cosmic Ray Intensity in the Stratosphere," in *Problems of the Physics of Cosmic Rays* (Nauka, Moscow, 1987), pp. 51–64 [in Russian].
11. ftp://ftp.ngdc.noaa.gov/STP/SOLAR_DATA
12. A. K. Lavrukhina, G. K. Ustinova, M. V. Alaniya, and L. I. Dorman, "Temporal, Radial, and Latitudinal Variations of GCR in the Solar System," Izv. Akad. Nauk SSSR, Ser. Fiz. **45**, 547–552 (1981).

13. A. K. Lavrukhina, G. K. Ustinova, M. V. Alania, and L. I. Dorman, "Temporal, Radial, and Latitudinal Variations of Galactic Cosmic Ray Gradients in the Solar System," in *Proceedings of 17th International Cosmic Ray Conference, Paris, France, 1981* (Paris, 1981), Vol. 3, pp. 238–241.
14. M. V. Alania, L. I. Dorman, A. K. Lavrukhina, and G. K. Ustinova, "GCR Variations in the Heliosphere According to Radioactivity of Meteorites," in *Proceedings of 18th International Cosmic Ray Conference, Bangalore, India, 1983* (Bangalore, 1983), Vol. 10, pp. 42–45.
15. A. K. Lavrukhina and G. K. Ustinova, *Meteorites as Probes of Cosmic Ray Variations* (Nauka, Moscow, 1990) [in Russian].
16. G. P. Lyubimov and N. V. Pereslegina, "Gradient of Cosmic Rays and Solar Activity" in *Cosmic Rays* (Nauka, Moscow, 1983), No. 22, pp. 97–104 [in Russian].
17. S. N. Vernov, A. N. Charakhch'yan, Yu. I. Stozhkov, and T. N. Charakhch'yan, Preprint No. 107, FIAN RAN (Fiz. Inst. Akad. Nauk, Moscow, 1974) [in Russian].
18. G. K. Ustinova, "Cosmic Rays in the Heliosphere and Cosmogenic Nuclides," Nucl. Geophys. **9**, 273–281 (1995).
19. G. K. Ustinova and A. K. Lavrukhina, "Cosmic Ray Variations in the Heliosphere Based on the Results of a Study of Extraterrestrial Materials," Geokhimiya, No. 4, 483–501 (1983).
20. V. A. Alexeev and G. K. Ustinova, "Characteristics of Galactic Cosmic Ray Modulation in 1954–1922 According to Meteorite Data," Izv. Akad. Nauk, Ser. Fiz. **63**, 1625–1629 (1999).
21. V. A. Alexeev, V. D. Gorin, and G. K. Ustinova, "Distribution and Variations of Galactic Cosmic Rays in the Heliosphere According to Meteorite Data," Dokl. Akad. Nauk **394**, 328–331 (2004).
22. L. Z. Rumshiskii, *Mathematical Processing of Experimental Results* (Nauka, Moscow, 1971) [in Russian].
23. R. B. McKibben, J. J. O'Gallagher, K. R. Pyle, and J. A. Simpson, "Cosmic Ray Intensity Gradients in the Outer Solar System Measured by Pioneer 10 and 11," in *Proceedings of 15th International Cosmic Ray Conference, Plovdiv, Bulgaria, 1977* (Plovdiv, 2001), Vol. 3, pp. 240–245.
24. A. K. Lavrukhina and G. K. Ustinova, "Determination of the Boundaries of a Modulation Region," Izv. Akad. Nauk SSSR, Ser. Fiz. **34**, 2401–2407 (1970).
25. A. K. Lavrukhina and G. K. Ustinova, "Gradient Variations of Cosmic Rays during the Solar Activity Cycle," Geomagn. Aeron. **12**, 744–746 (1972).
26. D. Venkatesan, R. B. Decker, and S. M. Krimigis, "Cosmic Ray Intensity Gradients during 1984–1986," in *Proceedings of 20th International Cosmic Ray Conference, Moscow, Russia, 1987* (Moscow, 1987), Vol. 3, pp. 385–388.
27. L. F. Burlaga, "Understanding the Heliosphere and Its Energetic Particles," in *Proceedings of 18th International Cosmic Ray Conference, Bangalore, India, 1983* (Bangalore, 1983), Vol. 12, pp. 21–60.
28. C. J. Hatton and G. A. Bowe, "An Empirical Model for the 11-Year Variation," in *Proceedings of 17th International Cosmic Ray Conference, Paris, France, 1981* (Paris, 1981), Vol. 3, pp. 255–258.
29. M. S. Potgieter and J. A. le Roux, "On a Possible Modulation Barrier in the Outer Heliosphere," in *Proceedings of 20th International Cosmic Ray Conference, Moscow, Russia, 1987* (Moscow, 1987), Vol. 3, pp. 291–294.
30. L. F. Burlaga and N. F. Ness, "Magnetic Field Strength Distributions and Spectra in the Heliosphere and Their Significance for Cosmic Ray Modulation: Voyager 1, 1980-1994," J. Geophys. Res. **103**, 29 719–29 732 (1998).
31. A. K. Lavrukhina and G. K. Ustinova, "Galactic Cosmic Ray Gradients in the Ecliptic Plane and at High Latitudes during Two Solar Cycles (Meteorite Data)," Adv. Space Res. **1** (3), 143–146 (1981).
32. H. S. Ahluwalia and I. V. Escobar, "The Cosmic Ray Intensity Variations and the Electromagnetic States of the Interplanetary Space," Geophys. Intern. **3** (2), 21–41 (1963).
33. Yu. I. Stozhkov, "Cosmic Ray Flux and Solar Magnetic Flow," Izv. Akad. Nauk, Ser. Fiz. **67**, 499–501 (2003).
34. R. Howard, "Studies of Solar Magnetic Fields," Solar Phys. **38**, 283–299 (1974).
35. M. B. Krainev, "Influence of the Total Solar Magnetic Field on an 11-year Cycle and 'Anomalous' Phenomena in Galactic Cosmic Rays," Izv. Akad. Nauk SSSR, Ser. Fiz. **47**, 1754–1760 (1983).
36. I. N. Toptygin, *Cosmic Rays in Interplanetary Magnetic Fields* (Nauka, Moscow, 1983; Reidel, Dordrecht, 1985).
37. http://quake.stanford.edu/~wso/Polar.ascii
38. V. I. Makarov and K. R. Sivaraman, "New Results Concerning the Global Solar Cycle," Solar Phys. **123**, 367–380 (1989).
39. Yu. I. Vitinskii, *Solar Activity* (Nauka, Moscow, 1983) [in Russian].
40. N. K. Pereyaslova, M. N. Nazarova, and I. E. Petrenko, "Solar Proton Events in the Near-Earth Space on the Growth Phase of a 23-Year Cycle of Solar Activity," Izv. Akad. Nauk, Ser. Fiz. **63**, 1579–1584 (1999).
41. Yu. I. Stozhkov, N. S. Svirzhevskii, and A. K. Svirzhevskaya, "Features of Long-Term Cosmic Ray Variations According to Atmospheric Measurements," Izv. Akad. Nauk, Ser. Fiz. **67**, 502–504 (2003).
42. G. K. Ustinova and A. K. Lavrukhina, "Latitude Gradients of Galactic Cosmic Rays from Radioactivity of Chondrites Including Pribram, Lost City and Innisfree," Meteoritics **14**, 554–559 (1979).
43. G. K. Ustinova, "Quasistationary Asymmetry of the GCR Density Distribution in the Heliosphere," in *Proceedings of 18th International Cosmic Ray Conference, Bangalore, India, 1983* (Bangalore, 1983), Vol. 10, pp. 71–74.
44. F. C. Jones, "Rapporteur Paper for Sessions MG1, MG3, and MG4. Modulation Theory, Interplanetary Propagation, and Interplanetary Acceleration," in *Proceedings of 18th International Cosmic Ray Conference, Bangalore, India, 1983* (Bangalore, 1983), Vol. 12, pp. 373–388.
45. http://nssdc.gsfc.nasa.gov/omniweb/form/dx1.html
46. http://quake.stanford.edu/~wso/wso.html

47. H. S. Ahluwalia, "Understanding Cosmic Ray Solar Modulation for Cycle 20," in *Proceedings of 28th International Cosmic Ray Conference, Tzukuba, Japan 2003* (Tzukuba, 2003), pp. 4035–4040.
48. B. M. Rubashev, *Problems of Solar Activity* (Nauka, Moscow, 1964) [in Russian].
49. Yu. I. Vitinskii, M. Kopetskii, and G. V. Kuklin, *Statistics of Spot-Forming Solar Activity* (Nauka, Moscow, 1986) [in Russian].
50. M. Waldmeier, "Der lange Sonnenzyklus," Zeitschr. Astrophys. **43** (2), 149–160 (1957).
51. Ya. B. Zel'dovich and A. A. Ruzmaikin, "Problems of a Dynamo in Astrophysics," Itogi Nauki Tekhn., Ser. Astron. **21**, 151–187 (1982).
52. http://www.clearlight.com/~mhieb/WVFossils/last_200_yrs.html
53. http://www.clearlight.com/~mhieb/WVFossils/temp_vs_CO_2.html
54. V. A. Granovskii and T. N. Siraya, *Methods of Experimental Data Processing during Measurements* (Energoatomizdat, Leningrad, 1990) [in Russian].